4

Machine Tool Dynamics and Vibrations

Yusuf Altintas
The University of British Columbia

4.1 Introduction

The accuracy of a machined part depends on the precision motion delivered by a machine tool under static, dynamic, and thermal loads. The accuracy is evaluated by measuring the discrepancy between the desired part dimensions identified on a part drawing and the actual part achieved after machining operations. The cutting tool deviates from a desired tool path due to errors in positioning the feed drives, thermal expansion of machine tool and workpiece structures, static and dynamic deformations of machine tool and workpiece, and misalignment of machine tool drives and spindle during assembly. Because the parts to be machined will vary depending on the end-user, the builder must design the machine tool structure and control of drives to deliver maximum accuracy during machining.

A machine tool system has three main groups of parts: mechanical structures, drives, and controls.

4.1.1 Mechanical Structure

The structure consists of stationary and moving bodies. The stationary parts carry moving bodies, such as table and spindle drives. They must be designed to carry large weights and absorb vibrations transmitted by the moving and rotating parts. The stationary parts are generally made of cast iron, concrete, and composites, which have high damping properties. The contact interface between the stationary and moving bodies can be selected from steel alloys that allow surface hardness in order to minimize wear.

4.1.2 Drives

In machine tools moving mechanisms are grouped into spindle and feed drives. The spindle drive provides sufficient angular speed, torque, and power to a rotating spindle shaft, which is held in

the spindle housing with roller or magnetic bearings. Spindle shafts with a medium-speed range are connected to the electric motor via belts. There may be a single-step gear reducer and a clutch between the electric motor and spindle shaft. High-speed spindles have electric motors built into the spindle in order to reduce the inertia and friction produced by the motor–spindle shaft coupling. The feed drives carry the table or the carriage. In general, the table is connected to the nut, and the nut houses a lead screw. The screw is connected to the drive motor either directly or via a gear system depending on the feed speed, inertia, and torque reduction requirements. High-speed machine tools may employ linear direct motors and drives without the feed screw and nut, thus avoiding excessive inertia and friction contact elements. The rotating parts such as feed screws and spindles are usually made of steel alloys, which have high elasticity, a surface-hardening property, and resistance against fatigue and cracks under dynamic, cyclic loads.

4.1.3 Controls

The control parts include servomotors, amplifiers, switches, and computers. The operator controls the motion of the machine from an operator panel of the CNC system.

Readers are referred to machine design handbooks and texts for the basics of designing stationary, linearly moving, and rotating shafts.[1] The principles of machine tool control can be found in dedicated texts.[2,3] The fundamentals of machine tool vibrations, which are unique to metal cutting, are covered in this handbook.

4.2 Chatter Vibrations in Cutting

Machine tool chatter vibrations occur due to a self-excitation mechanism in the generation of chip thickness during machining operations. One of the structural modes of the machine tool–workpiece system is excited initially by cutting forces. A wavy surface finish left during the previous revolution in turning, or by a previous tooth in milling, is removed during the succeeding revolution or tooth period and also leaves a wavy surface due to structural vibrations.[4] Depending on the phase shift between the two successive waves, the maximum chip thickness may exponentially grow while oscillating at a chatter frequency which is close to, but not equal to, a dominant structural mode in the system. The growing vibrations increase the cutting forces and may chip the tool and produce a poor, wavy surface finish. The self-excited chatter vibrations may be caused by mode coupling or regeneration of the chip thickness.[5] Mode-coupling chatter occurs when there are vibrations in two directions in the plane of cut. Regenerative chatter occurs due to phase differences between the vibration waves left on both sides of the chip, and occurs earlier than mode-coupling chatter in most machining cases. Hence, the fundamentals of regenerative chatter vibrations are explained in the following section using a simple, orthogonal cutting process as an example.

4.2.1 Stability of Regenerative Chatter Vibrations in Orthogonal Cutting

Consider a flat-faced orthogonal grooving tool fed perpendicular to the axis of cylindrical shaft held between the chuck and the tail stock center of a lathe (see Figure 4.1). The shaft is flexible in the direction of feed, and it vibrates due to feed cutting force (F_f). The initial surface of the shaft is smooth without waves during the first revolution, but the tool starts leaving wavy surface behind due to vibrations of the shaft in the feed direction y which is in the direction of radial cutting force (F_f). When the second revolution starts, the surface has waves both inside the cut where the tool is cutting (i.e., inner modulation, $y(t)$) and outside surface of the cut due to vibrations during the previous revolution of cut (i.e., outer modulation, $y(t - T)$). The resulting dynamic chip thickness $h(t)$ is no longer constant, but varying as a function of vibration frequency and the speed of the workpiece,

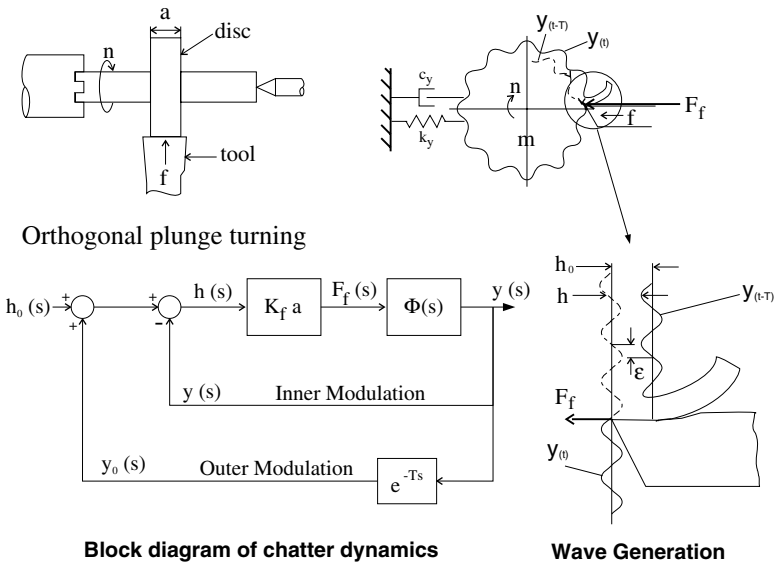

FIGURE 4.1 Mechanism of chatter vibrations in a plunge turning process.

$$h(t) = h_0 - [y(t) - y(t-T)] \tag{4.1}$$

where h_0 is the intended chip thickness which is equal to the feed rate of the machine. Assuming that the workpiece is approximated as a single degree-of-freedom system in the radial direction, the equation of motion of the system can be expressed as

$$\left.\begin{aligned} m_y y(t) + c_y y(t) + k_y y(t) = F_f(t) &= K_f a h(t) \\ &= K_f a[h_0 + y(t-T) - y(t)] \end{aligned}\right\} \tag{4.2}$$

where the feed cutting force $F_f(t)$ is proportional to the cutting constant in the feed direction (K_f), width of cut a, and the dynamic chip load $h(t)$. Because the forcing function on the right-hand side depends on the present and past solutions of vibrations ($y(t)$, $y(t-T)$) on the left side of the equation, the chatter vibration expression is a delay differential equation. The jumping of the tool due to excessive vibrations, and the influence of vibration marks left on the surface during the previous revolutions may further complicate the computation of exact chip thickness. The cutting constant K_f may change depending on the magnitude of instantaneous chip thickness and the orientation of the vibrating tool or workpiece, which is additional difficulty in the dynamic cutting process. When the flank face of the tool rubs against the wavy surface left behind, additional process damping is added to the dynamic cutting process which attenuates the chatter vibrations. The whole process is too complex and nonlinear to model correctly with analytical means, hence time-domain numerical methods are widely used to simulate the chatter vibrations in machining. However, a clear understanding of chatter stability is still important and best explained using a linear stability theory. The stability of chatter vibrations is analyzed using linear theory by Tobias,[6] Tlusty,[4] and Merritt.[7]

The chatter vibration system can be represented by the block diagram shown in Figure 4.1, where the parameters of the dynamic cutting process are shown in a Laplace domain. Input to the system is the desired chip thickness h_0, and the output of the feedback system is the current vibration $y(t)$ left on the inner surface. In the Laplace domain, $y(s) = \mathcal{L}y(t)$, and the vibration imprinted on the

outer surface during the previous revolution is $e^{-sT}y(s) = \mathcal{L}y(t-T)$ where T is the spindle period. The dynamic chip thickness in the Laplace domain is

$$h(s) = h_0 - y(s) + e^{-sT}y(s) = h_0 + (e^{-sT} - 1)y(s) \tag{4.3}$$

which produces dynamic cutting force,

$$F_f(s) = K_f\, ah(s) \tag{4.4}$$

The cutting force excites the structure and produces the current vibrations $y(s)$,

$$y(s) = F_f(s)\Phi(s) = K_f\, ah(s)\ \Phi(s) \tag{4.5}$$

where $\Phi(s)$ is the transfer function of the single degree of workpiece structure,

$$\Phi(s) = \frac{y(s)}{F_f(s)} = \frac{\omega_n^2}{k_y\left(s^2 + 2\zeta\omega_n s + \omega_n^2\right)}$$

Substituting $y(s)$ into $h(s)$ yields,

$$h(s) = h_0 + (e^{-sT} - 1)K_f\, ah(s)\Phi(s)$$

and the resulting transfer function between the dynamic and reference chip loads becomes,

$$\frac{h(s)}{h_0(s)} = \frac{1}{1 + (1 - e^{-sT})K_f\, a\Phi(s)} \tag{4.6}$$

The stability of the above close-loop transfer function is determined by the roots (s) of its characteristic equation, i.e.,

$$1 + (1 - e^{-sT)}\ K_f\, a\Phi(s) = 0$$

Let the root of the characteristic equation is $s = \sigma + j\omega_c$. If the real part of the root is positive ($\sigma > 0$), the time domain solution will have an exponential term with positive power (i.e., $e^{+|\sigma|t)}$. The chatter vibrations will grow indefinitely, and the system will be unstable. A negative real root ($\sigma < 0$) will suppress the vibrations with time (i.e., $e^{-|\sigma|t)}$, and the system is stable with chatter vibration-free cutting. When the real part is zero ($s = j\omega_c$), the system is critically stable, and the workpiece oscillates with constant vibration amplitude at chatter frequency ω_c. For critical borderline stability analysis ($s = j\omega_c$), the characteristic function becomes,

$$1 + (1 - e^{-j\omega_c T})K_f a_{lim}\Phi(j\omega_c) = 0 \tag{4.7}$$

where a_{lim} is the maximum axial depth of cut for chatter vibration free machining. The transfer function can be partitioned into real and imaginary parts, i.e., $\Phi(j\omega_c) = G + jH$. Rearranging the characteristic equation with real and complex parts yields,

$$\{1 + K_f a_{lim}[G(1 - \cos\omega_c T) - H\sin\omega_c T]\} + j\{K_f a_{lim}[G\sin\omega_c T + H(1 - \cos\omega_c T)]\} = 0$$

Both real and imaginary parts of the characteristic equation must be zero. If the imaginary part is considered first,

$$G\sin\omega_c T + H(1-\cos\omega_c T) = 0$$

and

$$\tan\psi = \frac{H(\omega_c)}{G(\omega_c)} = \frac{\sin\omega_c T}{\cos\omega_c T - 1} \tag{4.8}$$

where ψ is the phase shift of the structure's transfer function. Using the trigonometric identity cos $\omega_c T = \cos^2(\omega_c T/2) - \sin^2(\omega_c T/2)$ and sin $\omega_c T = 2\sin(\omega_c T/2)\cos(\omega_c T/2)$,

$$\tan\psi = \frac{\cos(\omega_c T/2)}{-\sin(\omega_c T/2)} = \tan[(\omega_c T)/2 - (3\pi)/2]$$

and

$$\omega_c T = 3\pi + 2\psi, \quad \psi = \tan^{-1}\frac{H}{G} \tag{4.9}$$

The spindle speed (n[*rev/s*]) and the chatter vibration frequency (ω_c) have a relationship which affects the dynamic chip thickness. Let's assume that the chatter vibration frequency is ω_c[*rad/s*] or f_c[*Hz*]. The number of vibration waves left on the surface of the workpiece is

$$f_c[\text{Hz}]\cdot T\,[\text{sec.}] = \frac{f_c}{n} = k + \frac{\epsilon}{2\pi} \tag{4.10}$$

where k is the integer number of waves and $\epsilon/2\pi$ is the fractional wave generated. The angle ϵ represents the phase difference between the inner and outer modulations. Note that if the spindle and vibration frequencies have an integer ratio, the phase difference between the inner and outer waves on the chip surface will be zero or 2π, hence the chip thickness will be constant albeit the presence of vibrations. In this case, the inner ($y(t)$) and outer ($y(t - T)$) waves are parallel to each other and there will be no chatter vibration. If the phase angle is not zero, the chip thickness changes continuously. Considering k integer number of full vibration cycles and the phase shift,

$$2\pi f_c\, T = 2k\pi + \epsilon \tag{4.11}$$

where the phase shift between the inner and outer waves is $\epsilon = 3\pi + 2\psi$. The corresponding spindle period (T[*sec*]) and speed (n[*rev/min*]) is found,

$$T = \frac{2k\pi + \epsilon}{2\pi f_c} \rightarrow n = \frac{60}{T} \tag{4.12}$$

The critical axial depth of the cut can be found by equating the real part of the characteristic equation to zero,

$$1 + K_f a_{lim}[G(1-\cos\omega_c T - H\sin\omega_c T] = 0$$

or

$$a_{lim} = \frac{-1}{K_f G[(1-\cos\omega_c T - (H/G)\sin\omega_c T]}$$

Substituting $H/G = (\sin \omega_c T)/(\cos \omega_c T - 1)$ and rearranging the above equation yields,

$$a_{lim} = \frac{-1}{2K_f G(\omega_c)} \tag{4.13}$$

Note that since the depth of cut is a physical quantity, the solution is valid only for the negative values of the real part of the transfer function ($G(\omega_c)$). The chatter vibrations may occur at any frequency where $G(\omega_c)$ is negative. If a_{lim} is selected using the minimum value of $G(\omega_c)$, the avoidance of chatter is guaranteed at any spindle speed. The expression indicates that the axial depth of cut is inversely proportional to the flexibility of the structure and cutting constant of the workpiece material. The harder the work material is, the larger the cutting constant K_f will be, thus reducing the chatter vibration-free axial depth of cut. Similarly, flexible machine tool or workpiece structures will also reduce the axial depth of cut or the *productivity.*

The above stability expression was first obtained by Tlusty.[4] Tobias[6] and Merrit[7] presented similar solutions. Tobias presented stability charts indicating chatter vibration-free spindle speeds and axial depth of cuts. Assuming that the transfer function of the structure at the cutting point (Φ) and cutting constant K_f are known or measured, the procedure of plotting the stability lobes can be summarized in the following:

- Select a chatter frequency (ω_c) at the negative real part of the transfer function.
- Calculate the phase angle of the structure at ω_c, Equation (4.8).
- Calculate the critical depth of cut from Equation (4.13).
- Calculate the spindle speed from Equation (4.12) for each stability lobe $k = 0, 1, 2, \ldots$.
- Repeat the procedure by scanning the chatter frequencies around the natural frequency of the structure.

If the structure has multiple degrees of freedom, an oriented transfer function of the system in the direction of chip thickness must be considered for Φ. In that case, the negative real part of the complete transfer function around all dominant modes must be scanned using the same procedure outlined for the orthogonal cutting process.

4.3 Analytical Prediction of Chatter Vibrations in Milling

The rotating cutting force and chip thickness directions, and intermittent cutting periods complicate the application of orthogonal chatter theory to milling operations. The following analytical chatter prediction model was presented by Altintas and Budak,[8,9] and provides practical guidance to machine tool users and designers for optimal process planning of depth of cuts and spindle speeds in milling operations.

4.3.1 Dynamic Milling Model

Milling cutters can be considered to have 2-orthogonal degrees of freedom as shown in Figure 4.2. The cutter is assumed to have N number of teeth with a zero helix angle. The cutting forces excite the structure in the feed (X) and normal (Y) directions, causing dynamic displacements x and y, respectively. The dynamic displacements are carried to rotating tooth number (j) in the radial or chip thickness direction with the coordinate transformation of $v_j = -x \sin \phi_j - y \cos \phi_j$ where ϕ_j is the instantaneous angular immersion of tooth (j) measured clockwise from the normal (Y) axis. If the spindle rotates at an angular speed of Ω (*rad/s*) the immersion angle varies with time as $\phi_j(t) = \Omega t$. The resulting chip thickness consists of static part ($s_t \sin \phi_j$), which is due to rigid body motion of the cutter, and the dynamic component caused by the vibrations of the tool at the present and

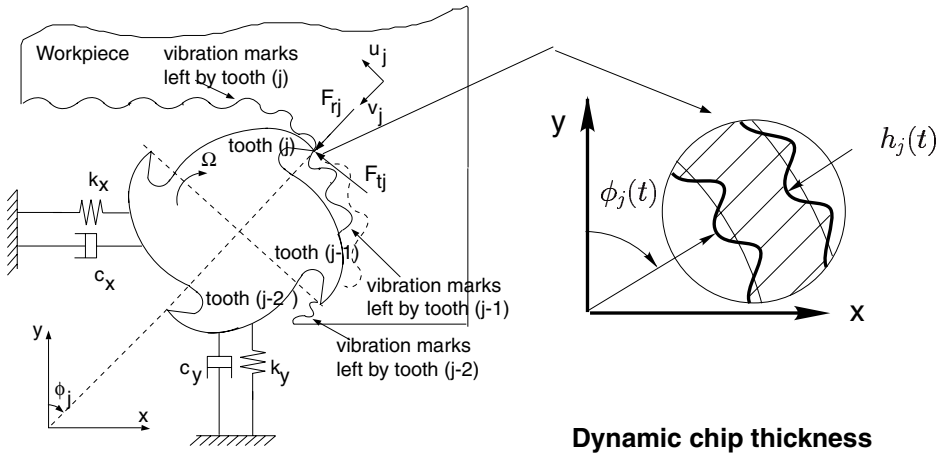

FIGURE 4.2 Mechanism of chatter in milling.

previous tooth periods. Because the chip thickness is measured in the radial direction (v_j), the total chip load can be expressed by,

$$h(\phi_j) = [s_t \sin \phi_j + (v_{j,0} - v_j)]g(\phi_j) \tag{4.14}$$

where s_t is the feed rate per tooth and ($v_{j,0}$, v_j) are the dynamic displacements of the cutter at the previous and present tooth periods, respectively. $g(\phi_j)$ is zero when the tool is out of cut, and unity otherwise

$$\left.\begin{aligned} g(\phi_j) &= 1 \leftarrow \phi_{st} < \phi_j < \phi_{ex} \\ g(\phi_j) &= 0 \leftarrow \phi_j < \phi_{st} \; or \; \phi_j > \phi_{ex}. \end{aligned}\right\} \tag{4.15}$$

where ϕ_{st}, ϕ_{ex} are start and exit immersion angles of the cutter to and from the cut, respectively. Henceforth, the static component of the chip thickness ($s_t \sin \phi_j$) is dropped from the expressions because it does not contribute to the dynamic chip load regeneration mechanism. Substituting v_j into (4.14) yields,

$$h(\phi_j) = [\Delta x \sin \phi_j + \Delta y \cos \phi_j]g(\phi_j) \tag{4.16}$$

where $\Delta x = x - x_0$, $\Delta y = y - y_0$. (x, y) and (x_0, y_0) represent the dynamic displacements of the cutter structure at the present and previous tooth periods, respectively. The tangential (F_{tj}) and radial (F_{rj}) cutting forces acting on the tooth j is proportional to the axial depth of cut (a) and chip thickness (h),

$$F_{tj} = K_t a h(\phi_j), \quad F_{rj} = K_r F_{tj} \tag{4.17}$$

where cutting coefficients K_t and K_r are constant. Resolving the cutting forces in the x and y directions,

$$F_{xj} = -F_{tj}\cos\phi_j - F_{rj}\sin\phi_j$$
$$F_{yj} = +F_{tj}\sin\phi_j - F_{rj}\cos\phi_j \tag{4.18}$$

and summing the cutting forces contributed by all teeth, the total dynamic milling forces acting on the cutter are found as

$$F_x = \sum_{j=0}^{N-1} F_{x_j}(\phi_j) \quad ; \quad F_y = \sum_{j=0}^{N-1} F_{y_j}(\phi_j) \tag{4.19}$$

where $\phi_j = \phi + j\phi_p$, and cutter pitch angle is $\phi_p = 2\pi / N$. Substituting the chip thickness (4.16) and tooth forces (4.7) into (4.18), and rearranging the resulting expressions in matrix form yields,

$$\begin{Bmatrix} F_x \\ F_y \end{Bmatrix} = \frac{1}{2} a K_t \begin{bmatrix} a_{xx} & a_{xy} \\ a_{yx} & a_{yy} \end{bmatrix} \begin{Bmatrix} \Delta x \\ \Delta y \end{Bmatrix} \tag{4.20}$$

where time-varying directional dynamic milling force coefficients are given by

$$a_{xx} = \sum_{j=0}^{N-1} -g_j[\sin 2\phi_j + K_r(1-\cos 2\phi_j)]$$

$$a_{xy} = \sum_{j=0}^{N-1} -g_j[(1+\cos 2\phi_j) + K_r \sin 2\phi_j]$$

$$a_{yx} = \sum_{j=0}^{N-1} g_j[(1-\cos 2\phi_j) - K_r \sin 2\phi_j]$$

$$a_{yy} = \sum_{j=0}^{N-1} g_j[\sin 2\phi_j - K_r(1+\cos 2\phi_j)]$$

Considering that the angular position of the parameters changes with time and angular velocity, Equation (4.20) can be expressed in time domain in a matrix form as[10,11]

$$\{F(t)\} = \frac{1}{2} a K_t [A(t)]\{\Delta(t)\} \tag{4.21}$$

As the cutter rotates, the directional factors vary with time, which is the fundamental difference between milling and operations like turning, where the direction of the force is constant. However, like the milling forces, $[A(t)]$ is periodic at tooth passing frequency $\omega = N\Omega$ or tooth period $T = 2\pi/\omega$, thus can be expanded into Fourier series.

$$[A(t)] = \sum_{r=-\infty}^{\infty} [A_r] e^{ir\omega t}, \qquad [A_r] = \frac{1}{T}\int_0^T [A(t)\,|\, e^{-ir\omega t} dt \tag{4.22}$$

The number of harmonics (r) of the tooth-passing frequency (ω) to be considered for an accurate reconstruction of $[A(t)]$ depends on the immersion conditions and the number of teeth in the cut. If the most simplistic approximation, the average component of the Fourier series expansion, is considered, i.e., $r = 0$,

$$[A_0] = \frac{1}{T}\int_0^T [A(t)dt. \tag{4.23}$$

Because $[A_0]$ is valid only between the entry (ϕ_{st}) and exit (ϕ_{ex}) angles of the cutter (i.e., $g_j(\phi_j) = 1$), and $\phi_j = \Omega\, t$ and $\phi_p = \Omega\, T$, it becomes equal to the average value of $[A(t)]$ at cutter pitch angle $\phi_p = 2\pi / N$.

$$[A(0)] = \frac{1}{\phi_p}\int_{\phi_{st}}^{\phi_{ex}} [A(\phi)]d\phi = \frac{N}{2\pi}\begin{bmatrix} \alpha_{xx} & \alpha_{xy} \\ \alpha_{yx} & \alpha_{yy} \end{bmatrix} \tag{4.24}$$

where the integrated functions are given as

$$\alpha_{xx} = \tfrac{1}{2}\left[\cos 2\phi - 2K_r\phi + K_r \sin 2\phi\right]_{\phi_{st}}^{\phi_{ex}}$$

$$\alpha_{xy} = \tfrac{1}{2}\left[-\sin 2\phi - 2\phi + K_r \cos 2\phi\right]_{\phi_{st}}^{\phi_{ex}}$$

$$\alpha_{yx} = \tfrac{1}{2}\left[-\sin 2\phi + 2\phi + K_r \cos 2\phi\right]_{\phi_{st}}^{\phi_{ex}}$$

$$\alpha_{yy} = \tfrac{1}{2}\left[-\cos 2\phi - 2K_r\phi - K_r \sin 2\phi\right]_{\phi_{st}}^{\phi_{ex}}$$

The average directional factors are dependent on the radial cutting constant (K_r) and the width of cut bound by entry (ϕ_{st}) and exit (ϕ_{ex}) angles. The dynamic milling expression (4.21) is reduced to the following

$$\{F(t)\} = \frac{1}{2} a K_t [A_0]\{\Delta(t)\} \tag{4.25}$$

where $[A_0]$ is a time-invariant but immersion-dependent directional cutting coefficient matrix. Because the average cutting force-per-tooth period is independent of the helix angle, $[A_0]$ is valid for helical end mills as well.

4.3.2 Chatter Stability Lobes

Transfer function matrix ($[\Phi\ (i\omega)]$) identified at the cutter–workpiece contact zone,

$$[\Phi(i\omega)] = \begin{bmatrix} \Phi_{xx}(i\omega) & \Phi_{xy}(i\omega) \\ \Phi_{yx}(i\omega) & \Phi_{yy}(i\omega) \end{bmatrix} \tag{4.26}$$

where $\Phi_{xx}(i\omega)$ and $\Phi_{yy}(i\omega)$ are the direct transfer functions in the x and y directions, and $\Phi_{xy}(i\omega)$ and $\Phi_{yx}(i\omega)$ are the cross-transfer functions. The vibration vectors at the present time (t) and previous tooth period ($t - T$) are defined as,

$$\{r\} = \{x(t)\ y(t)\}^T\ ;\{r_0\} = \{x(t-T)\ y(t-T)\}^T.$$

Describing the vibrations at the chatter frequency ω_c in the frequency domain using harmonic functions,

$$\left.\begin{aligned}\{r(i\omega_c)\} &= [\Phi(i\omega)]\{F\}e^{i\omega_c t}\\ \{r_0(i\omega_c)\} &= e^{-i\omega_c t}\{r(i\omega_c)\}\end{aligned}\right\} \tag{4.27}$$

and substituting $\{\Delta\} = \{(x - x_0\}\ (y - y_0)\}^T$ gives,

$$\begin{aligned}\{\Delta(i\omega_c)\} &= \{r(i\omega_c)\} - \{r_0(i\omega_c)\}\\ &= [1 - e^{-i\omega_c T}]e^{i\omega_c t}[\Phi(i\omega_c)]\{F\}\end{aligned}$$

where $\omega_c T$ is the phase delay between the vibrations at successive tooth periods T. Substituting $\{\Phi(i\omega_c)\}$ into the dynamic milling Equation (4.25) gives

$$\{F\}e^{i\omega_c t} = \frac{1}{2}aK_t[1 - e^{-i\omega_c T}][A_0][\Phi(i\omega_c)]\{F\}e^{i\omega_c t}$$

which has a nontrivial solution if its determinant is zero,

$$\det[[I] - \frac{1}{2}K_t a(1 - e^{i\omega_c T})[A_0][\Phi(i\omega_c)]] = 0$$

which is the characteristic equation of the closed-loop dynamic milling system. The notation is further simplified by defining the oriented transfer function matrix as

$$[\Phi_0(i\omega_c)] = \begin{bmatrix}\alpha_{xx}\Phi_{xx}(i\omega_c) + \alpha_{xy}\Phi_{yx}(i\omega_c) & \alpha_{xx}\Phi_{xy}(i\omega_c) + \alpha_{xy}\Phi_{yy}(i\omega_c)\\ \alpha_{yx}\Phi_{xx}(i\omega_c) + \alpha_{yy}\Phi_{yx}(i\omega_c) & \alpha_{yx}\Phi_{xy}(i\omega_c) + \alpha_{yy}\Phi_{yy}(i\omega_c)\end{bmatrix} \tag{4.28}$$

and the eigenvalue of the characteristic equation as

$$\Lambda = -\frac{N}{4\pi}aK_t(1 - e^{-i\omega_c T}). \tag{4.29}$$

The resulting characteristic equation becomes,

$$\det[[I] + \Lambda[\Phi_0(i\omega_c)]] = 0 \tag{4.30}$$

The eigenvalue of the above equation can easily be solved for a given chatter frequency ω_c, static cutting coefficients (K_t, K_r) which can be stored as a material-dependent quantity for any milling cutter geometry, radial immersion (ϕ_{st}, ϕ_{ex}), and transfer function of the structure (4.28). If two orthogonal degrees-of-freedom in feed (X) and normal (Y) directions are considered (i.e., $\Phi_{xy} = \Phi_{yx} = 0.0$), the characteristic equation becomes just a quadratic function

$$a_0\Lambda^2 + a_1\Lambda + 1 = 0 \tag{4.31}$$

where

$$a_0 = \Phi_{xx}(i\omega_c)\Phi_{yy}(i\omega_c)(\alpha_{xx}\alpha_{yy} - \alpha_{xy}\alpha_{yx})$$

$$a_1 = \alpha_{xx}\Phi_{xx}(i\omega_c) + \alpha_{yy}\Phi_{yy}(i\omega_c)$$

Then, the eigenvalue Ω is obtained as

$$\Lambda = -\frac{1}{2a_0}(a_1 \pm \sqrt{a_1^2 - 4a_0}). \tag{4.32}$$

As long as the plane of cut (x, y) is considered, the characteristic equation is still a simple quadratic function regardless of the number of modes considered in the machine tool structure. Indeed, the actual transfer function measurements of the machine dynamics can be used at each frequency. Because the transfer functions are complex, the eigenvalue has a real and an imaginary part, $\Lambda = \Lambda_R + i\Lambda_I$. Substituting the eigenvalue and $e^{-i\omega_c T} = \cos\omega_c T - i\sin\omega_c T$ in Equation (4.29) gives the critical axial depth of cut at chatter frequency ω_c,

$$a_{lim} = -\frac{2\pi}{NK_t}\left[\frac{\Lambda_R(1-\cos\omega_c T) + \Lambda_I \sin\omega_c T}{(1-\cos\omega_c T)} + i\frac{\Lambda_I(1-\cos\omega_c T) - \Lambda_R \sin\omega_c T}{(1-\cos\omega_c T)}\right] \tag{4.33}$$

Because a_{lim} is a real number, the imaginary part of the Equation (4.33) must vanish,

$$\Lambda_I(1-\cos\omega_c T) - \Lambda_R \sin\omega_c T = 0 \tag{4.34}$$

By substituting,

$$\kappa = \frac{\Lambda_I}{\Lambda_R} = \frac{\sin\omega_c T}{1-\cos\omega_c T} \tag{4.35}$$

into the real part of the Equation (4.33) (imaginary part vanishes), the final expression for chatter-free axial depth of cut is found as

$$a_{\lim} = -\frac{2\pi\Lambda_R}{NK_t}(1+\kappa^2) \tag{4.36}$$

Therefore, given the chatter frequency (ω_c), the chatter limit in terms of the axial depth of cut can directly be determined from Equation (4.36).

The corresponding spindle speeds are also found in a manner similar to the chatter in orthogonal cutting presented in the previous section.

From Equation 4.35,

$$\kappa = \tan\psi = \frac{\cos(\omega_c T/2)}{\sin(\omega_c T/2)} = \tan[\pi/2 - (\omega_c T/2)] \tag{4.37}$$

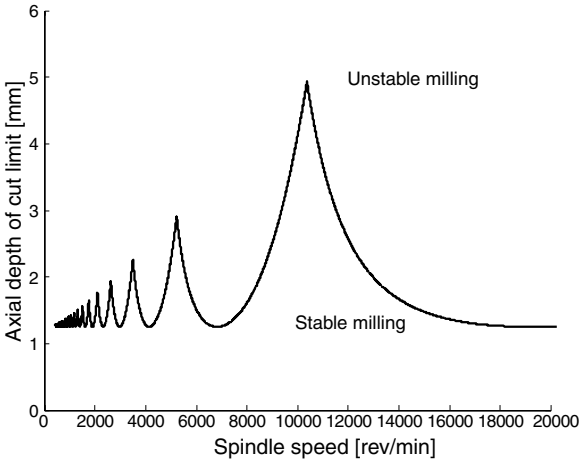

FIGURE 4.3 Stability lobes for a half immersion down milling of Al7075-T6 material with a bullnose cutter having two edges, 31.75 shank diameter and 4.7625-mm corner radius. The feed per tooth was $s_t = 0.050$ *mm*/rev in cutting tests.

and the phase shift of the eigenvalue is $\psi = \tan^{-1}\kappa$, and $\in = \pi - 2\psi$ is the phase shift between inner and outer modulations (present and previous vibration marks). Thus, if k is the integer number of full vibration waves (i.e., lobes) imprinted on the cut arc,

$$\omega_c T = \in + 2k\pi \tag{4.38}$$

Again, care must be taken in calculating the phase shift (ψ) from the real (Λ_R) and imaginary (Λ_I) parts of the eigenvalue. The spindle speed n(*rev/min*) is simply calculated by finding the tooth-passing period T(s),

$$T = \frac{1}{\omega_c}(\in + 2k\pi) \rightarrow n = \frac{60}{NT} \tag{4.39}$$

In summary, the transfer functions of the machine tool system are identified, and the dynamic cutting coefficients are evaluated from the derived Equation (4.24) for a specified cutter, workpiece material, and radial immersion of the cut. Then the stability lobes are calculated as follows:[8]

- Select a chatter frequency from transfer functions around a dominant mode.
- Solve the eigenvalue Equation (4.31).
- Calculate the critical depth of cut from Equation (4.36).
- Calculate the spindle speed from Equation (4.39) for each stability lobe $k = 0, 1, 2, \ldots$.
- Repeat the procedure by scanning the chatter frequencies around all dominant modes of the structure evident on the transfer functions.

A sample stability lobe for a vertical machining center milling Aluminum 7075 alloy with a four-fluted helical end mill is shown in Figure 4.3. The measured transfer function parameters of the machine at the tool tip are given as follows: $\omega_{nx} = \{452.8, 1448\}Hz$; $\zeta_x = \{0.12, 0.017\}$, $k_x = \{124.7E + 6, (-) 6595.6E + 6\}N/m$; $\omega_{ny} = \{516, 1407\}Hz$; $\zeta_x = \{0.024, 0.0324\}$, $k_y = \{(-) 2.7916E + 10, 3.3659E + 9\}N/m$ in the feed (x) and normal (y) directions, respectively. The stability lobes are predicted analytically with the theory given here, as well as using a time domain numerical solution which takes a considerable amount of computation time. The analytical method agrees well with the numerical solutions. The machine tool exhibits severe chatter vibrations when the

spindle speed is set to 9500 rev/min. The cutting force amplitudes are large, and the chatter occurs at 1448 Hz, which is the second bending mode of the spindle. When the speed and, therefore, productivity are increased to 14,000 rev/min, the chatter disappears and the force is dominated by the regular tooth-passing frequency of 467 Hz. The finish surface becomes acceptable, and the cutting force magnitude drops at the chatter vibration-free spindle speed and depth of cut.

References

1. F. Koenigsberger and J. Tlusty, *Machine Tool Structures, Vol. I: Stability against Chatter,* Pergamon Press, Oxford, 1967.
2. Y. Koren, *Computer Control of Manufacturing Systems,* McGraw Hill, New York, 1983.
3. Y. Altintas, *Manufacturing Automation: Metal Cutting Mechanics, Machine Tool Vibrations, and CNC Design,* Cambridge University Press, Cambridge, 2000.
4. J. Tlusty and M. Polacek, The stability of machine tools against self-excited vibrations in machining, *International Research in Production Engineering,* ASME, 465–474, 1963.
5. S.A. Tobias and W. Fishwick, *Theory of Regenerative Chatter,* The Engineer, London, 1958.
6. S.A Tobias, *Machine Tool Vibrations,* Blackie and Sons Ltd., London, 1965.
7. H.E. Merrit, Theory of self-excited machine tool chatter, *Transactions of ASME Journal of Engineering for Industry,* 87, 447–454, 1965.
8. Y. Altintas and E. Budak, Analytical prediction of stability lobes in milling, *Annals of the CIRP,* 44(1), 357–362, 1995.
9. E. Budak and Y. Altintas, Analytical prediction of chatter stability conditions for multi-degree of systems in milling. Part i: Modelling, Part ii: Applications, *Transactions of ASME Journal of Dynamic Systems, Measurement and Control,* 120, 22–36, 1998.
10. R.E. Hohn, R. Sridhar, and G.W. Long, A stability algorithm for a special case of the milling process, *Transactions of ASME Journal of Engineering for Industry,* 325–329, May 1968.
11. I. Minis, T. Yanushevsky, R. Tembo, and R. Hocken, Analysis of linear and nonlinear chatter in milling, *Annals of the CIRP,* 39, 459–462, 1990.